Supplementary Information

Modulated Hydrothermal Synthesis of Highly Stable MOF-808(Hf) for Methane Storage

Zhigang Hu,*[,†,‡] Tanay Kundu,[‡] Yuxiang Wang,[‡] Yao Sun,[#,§] Kaiyang Zeng,[#] and Dan Zhao*[,‡]

[†] Department of Chemical Engineering, Brunel University London, Kingston Lane, Uxbridge, UB8 3PH, United Kingdom

[‡] Department of Chemical & Biomolecular Engineering, National University of Singapore, 4 Engineering Drive 4, 117585, Singapore

[#] Department of Mechanical Engineering, National University of Singapore, 9 Engineering Drive 1, 117576, Singapore

[§] School of Science, Harbin Institute of Technology, Shenzhen, 518055, China

Correspondence and requests for materials should be addressed to:
Zhigang Hu (E-mail: zhigang.hu@brunel.ac.uk)
Dan Zhao (E-mail: chezhao@nus.edu.sg)

This supporting material contains **25** pages, including **14** figures, and **4** tables.

Table of Contents

1. Materials and Methods

All the reagents were obtained from commercial suppliers and used without further purification. Field-emission scanning electron microscope (FE-SEM) analyses were conducted on a FEI Quanta 600 SEM (20 kV) equipped with an energy dispersive spectrometer (EDS, Oxford Instruments, 80 mm^2 detector). Samples were treated via Pt sputtering before observation. Elemental analyses (EA) were performed on a Vario MICRO series CHNOS Elemental Analyzer. Powder X-ray diffraction patterns were obtained on a Bruker D8 Advance X-ray Powder Diffractometer equipped with a Cu sealed tube (λ = 1.54178 Å) at a scan rate of 0.02 ° s^{-1}. Thermogravimetric analyses (TGA) were performed using a Shimadzu DTG-60AH Thermal Analyzer under flowing N_2 or air, with a heating rate of 10 °C min^{-1}. The MOF powder was mechanically tapped inside a glass measuring cylinder until there was no change in the volume of the product to calculate the tap density.[1]

2. Low-Pressure Gas Sorption Measurements

Gas sorption isotherms were measured up to 1 bar using a Micromeritics ASAP 2020 surface area and pore size analyzer. Before the measurements, the samples (~50 mg) were degassed under reduced pressure (< 10^{-2} Pa) at 150 °C for 12 h. UHP grade N_2, He, H_2, CH_4, and CO_2 were used for all the measurements. Oil-free vacuum pumps and oil-free pressure regulators were used to prevent contamination of the samples during the degassing process and isotherm measurement. The temperatures of 77 K, 87 K, 273 K, and 298 K were maintained with a liquid nitrogen bath, a liquid argon bath, an ice water bath, and under room temperature, respectively. Pore size distribution data were calculated from the N_2 sorption isotherms at 77 K based on non-local density functional theory (NLDFT) model (assuming slit pore geometry) and Barrett-Joyner-Halenda (BJH) desorption model in the Micromeritics ASAP 2020 software package.

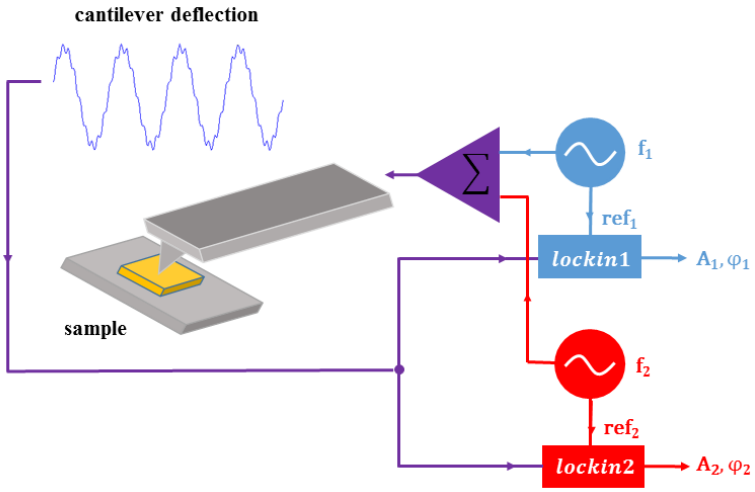

Figure S1. Schematic illustration of the AM-FM mode: the 1st mode amplitude is controlled to create the topography of the sample while the 2nd mode frequency is to calculate tip-sample stiffness and elasticity.

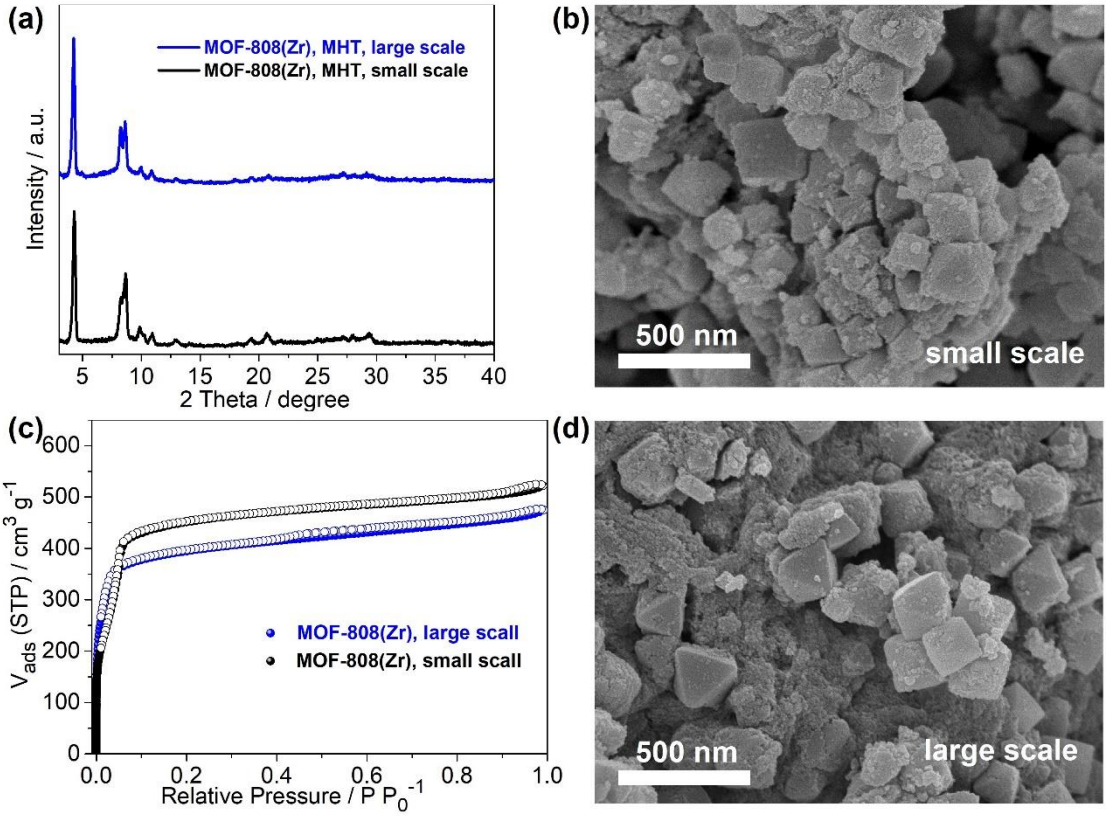

Figure S2. PXRD patterns (a), FE-SEM images (b, d), and N_2 isotherms (c) of MOF-808(Zr) synthesized in small and large scale.

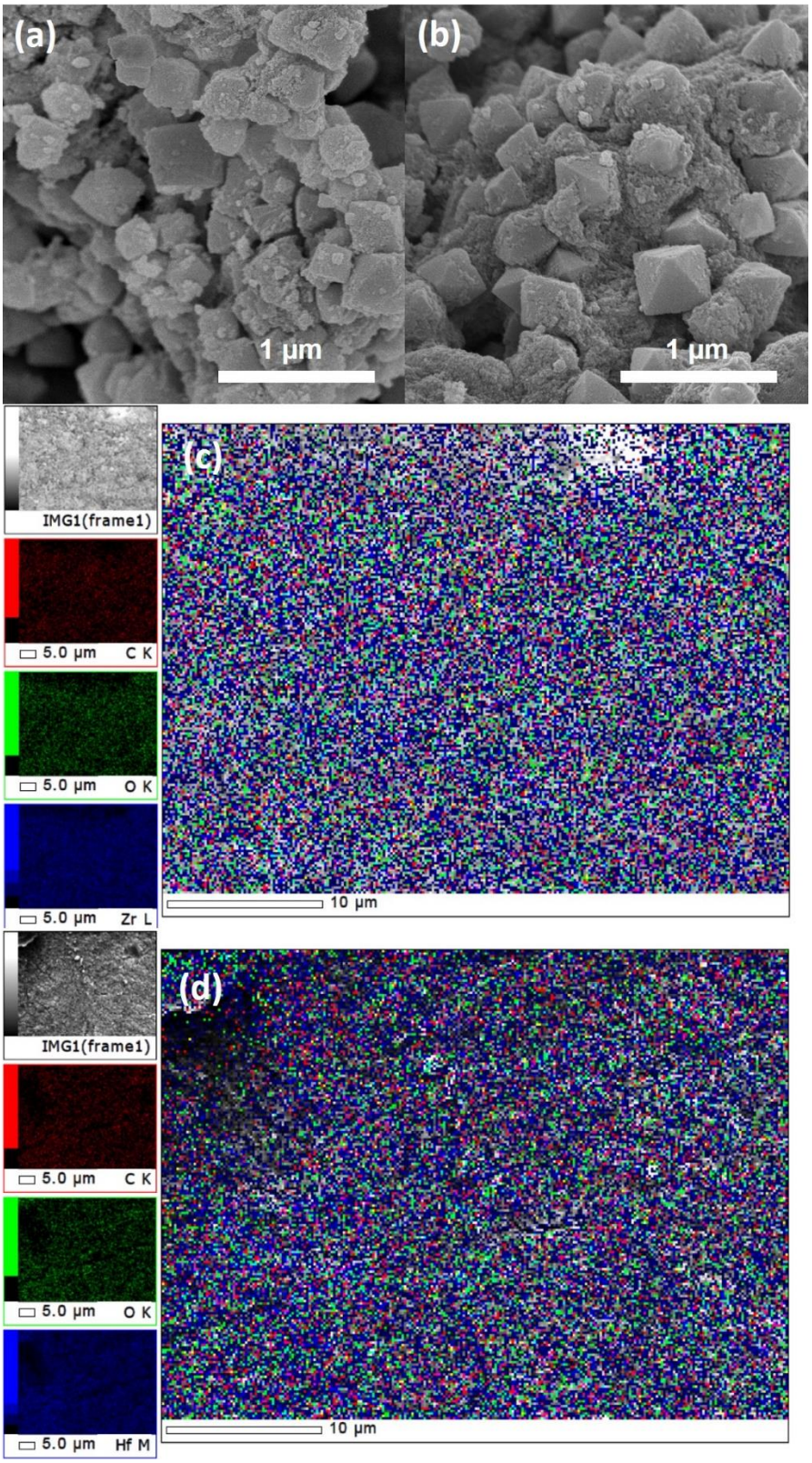

Figure S3. FE-SEM images: (a) MOF-808(Zr); (b) MOF-808(Hf). EDS-mapping images: (c) MOF-808(Zr); (d) MOF-808(Hf). Blue, metal; red, carbon; green, oxygen.

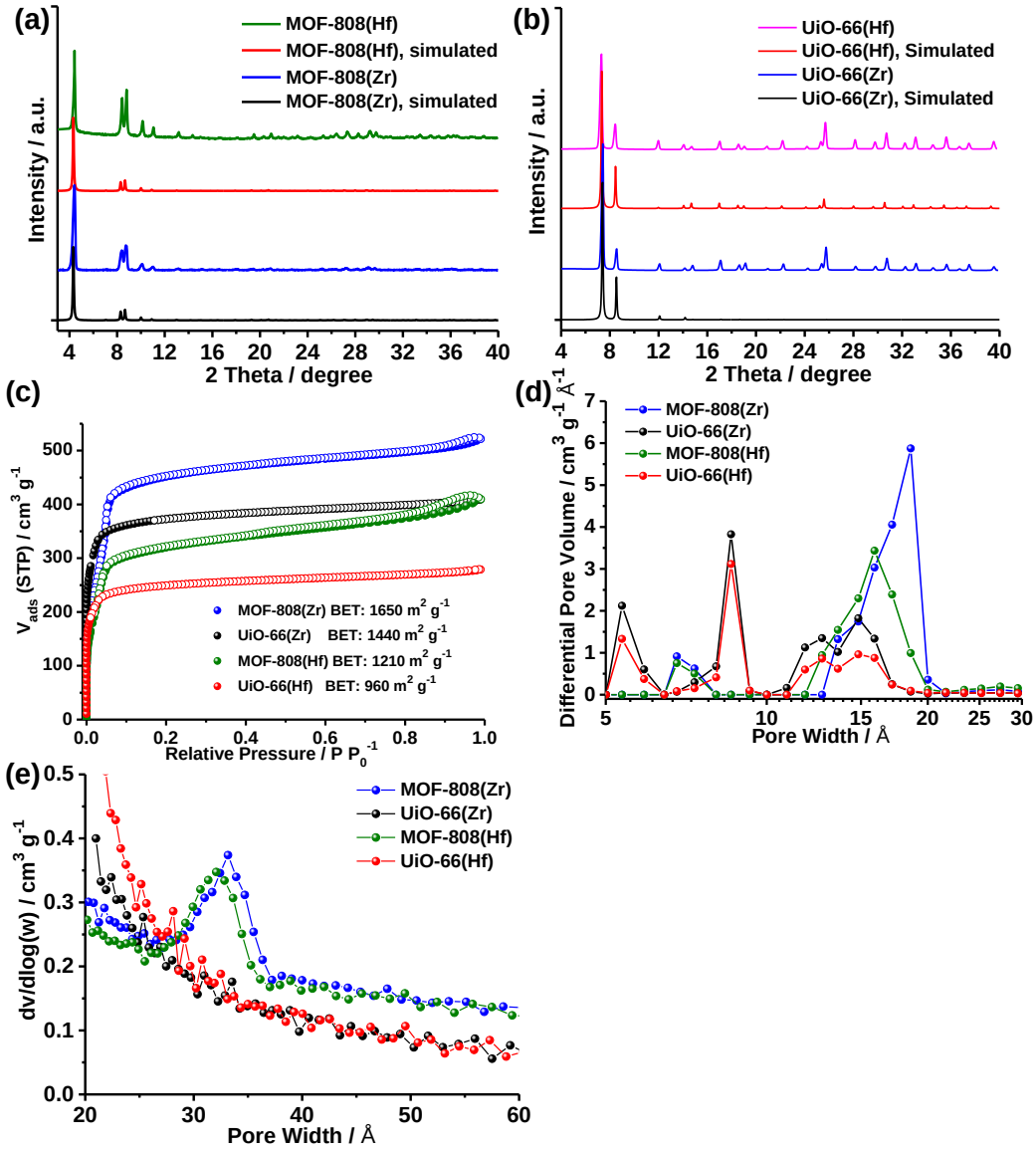

Figure S4. Characterizations of MOF-808 and UiO-66: (a, b) Powder X-ray diffraction (PXRD) patterns; (c) N_2 sorption isotherms at 77 K; (d) Pore size distribution calculated from non-local density functional theory (NLDFT) model (assuming slit pore geometry); (e) Pore size distribution calculated from Barrett-Joyner-Halenda (BJH) desorption model.

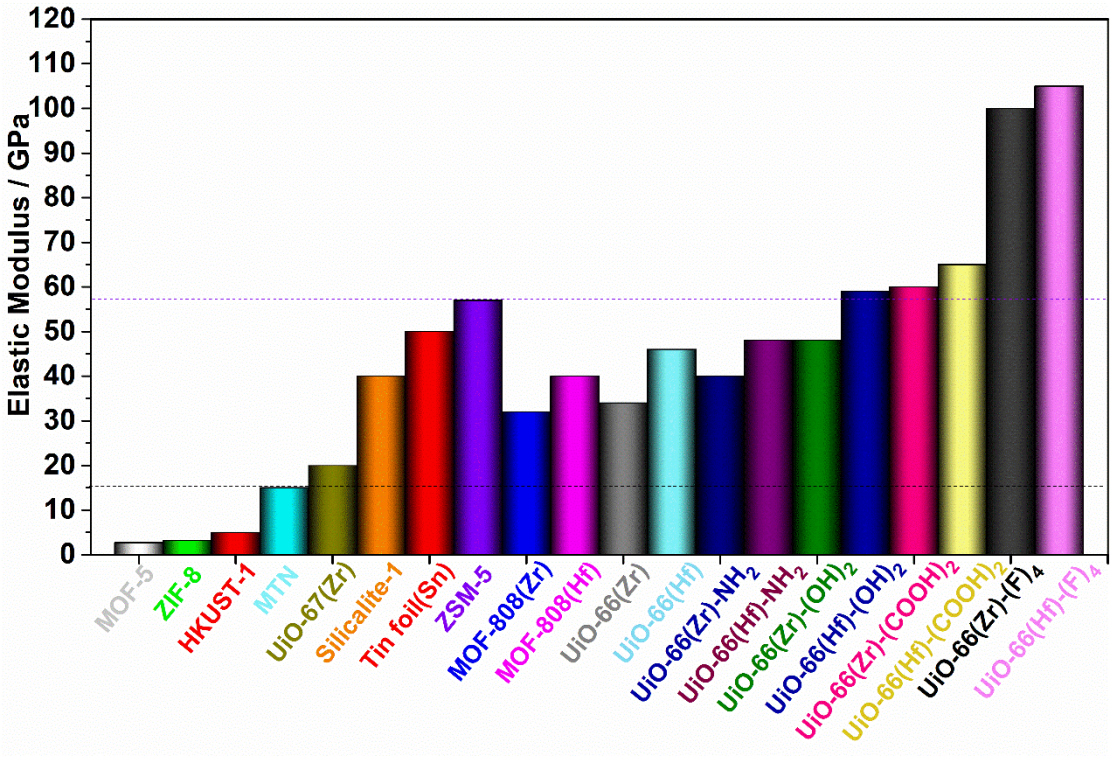

Figure S5. Summary of elastic moduli of representative materials.

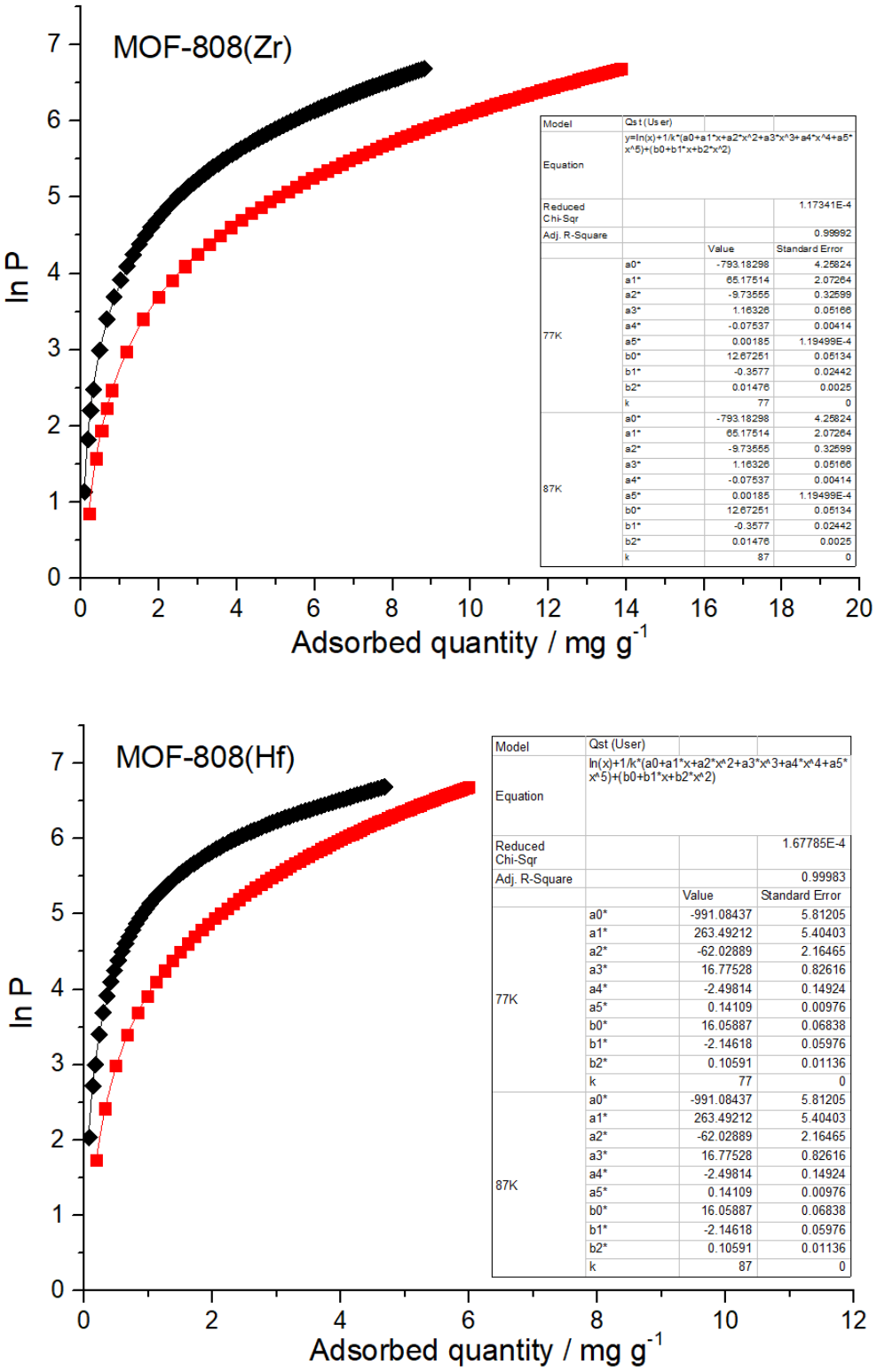

Figure S6. Virial fitting of H_2 sorption isotherms at 77 K and 87 K.

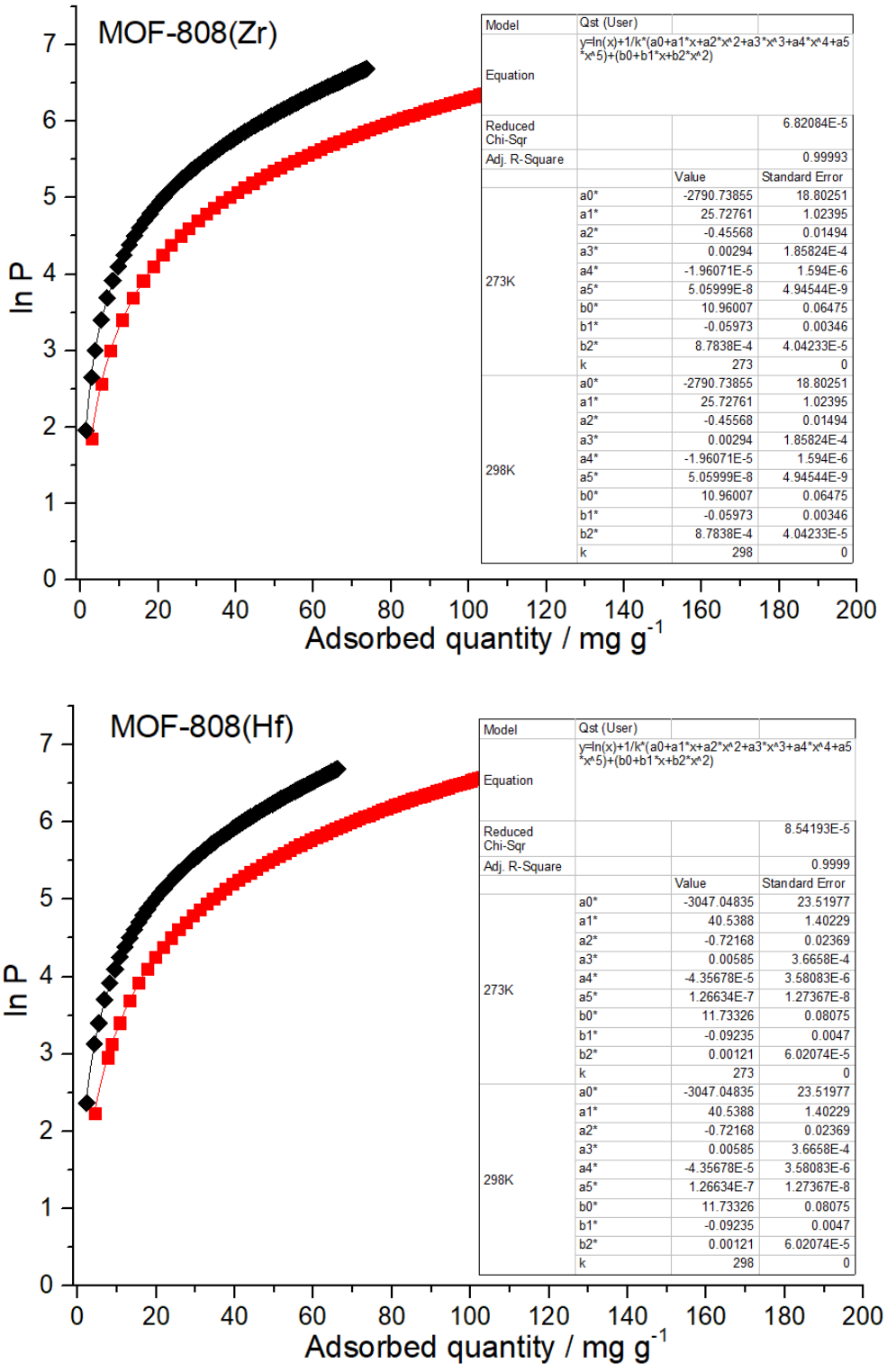

Figure S7. Virial fitting of CO_2 sorption isotherms at 273 K and 298 K.

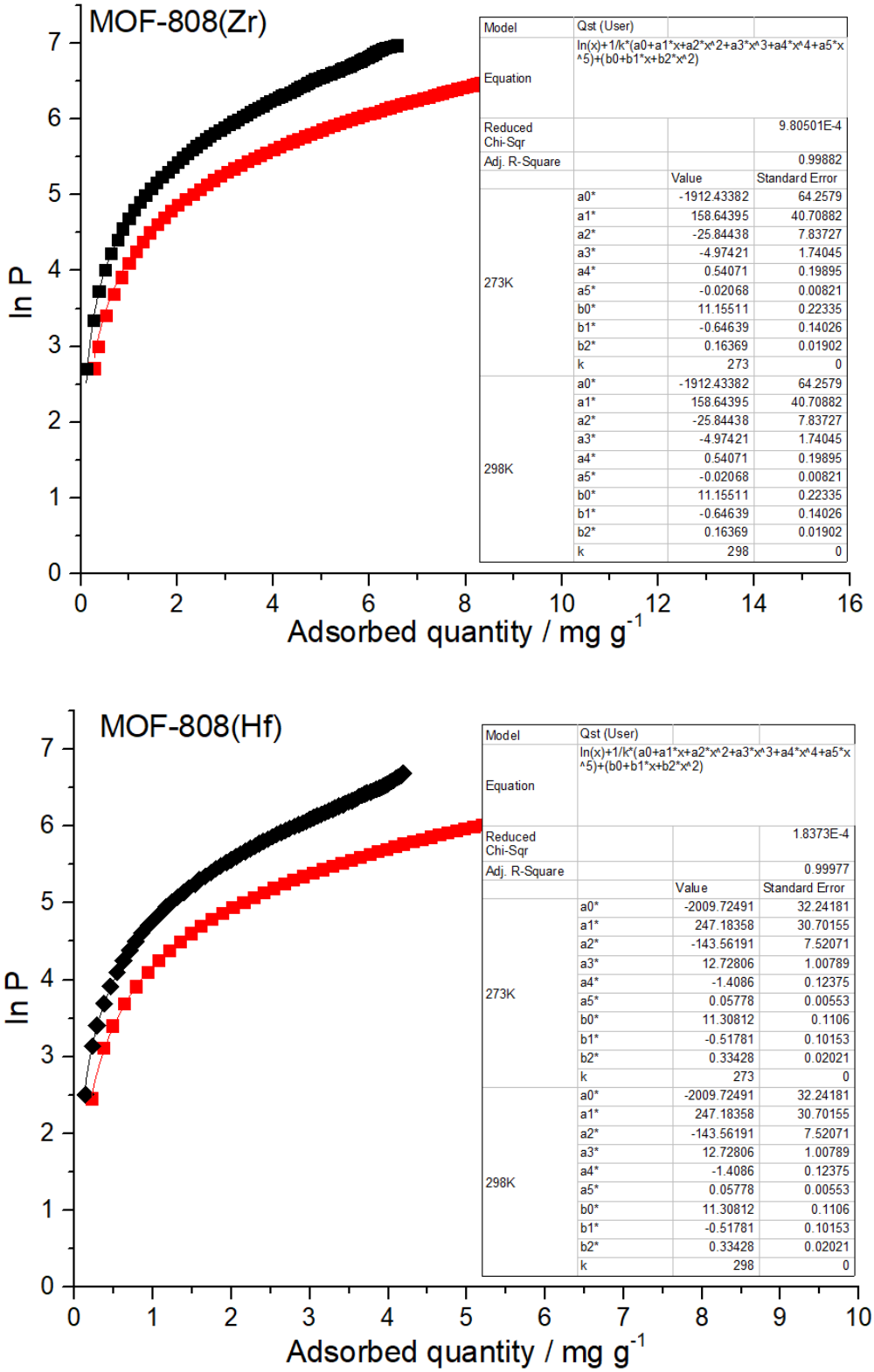

Figure S8. Virial fitting of CH_4 sorption isotherms at 273 K and 298 K.

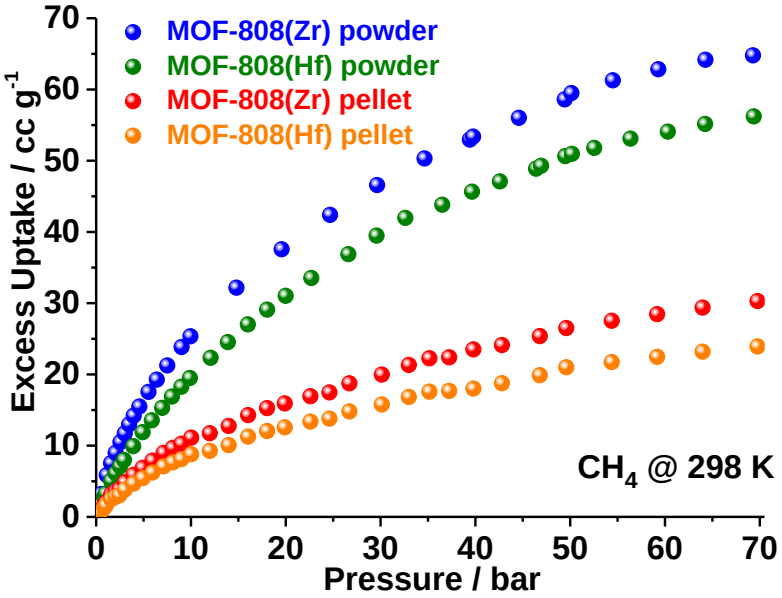

Figure S9. High-pressure gravimetric excess CH_4 sorption isotherms of MOF-808 powder and pellet at 298 K.

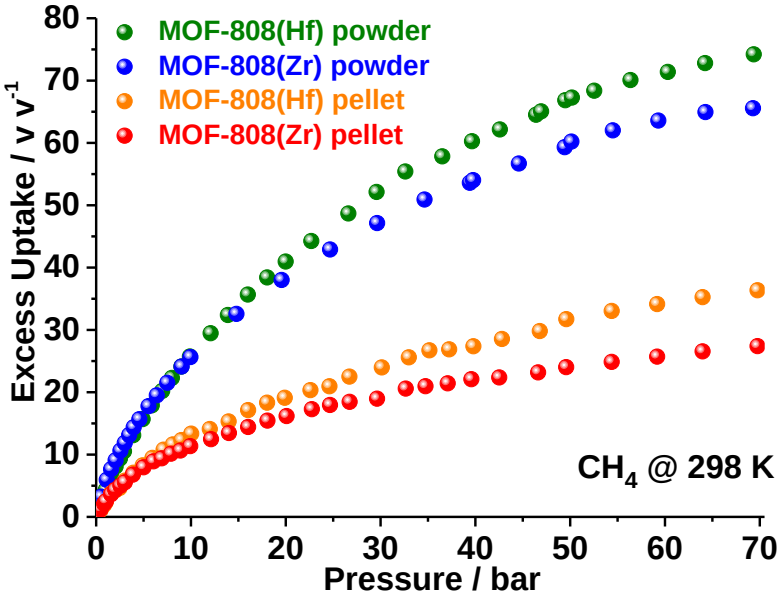

Figure S10. High-pressure volumetric excess CH_4 sorption isotherms of MOF-808 powder and pellet at 298 K. Volumetric uptake capacities are calculated by tap and pellet densities, respectively.

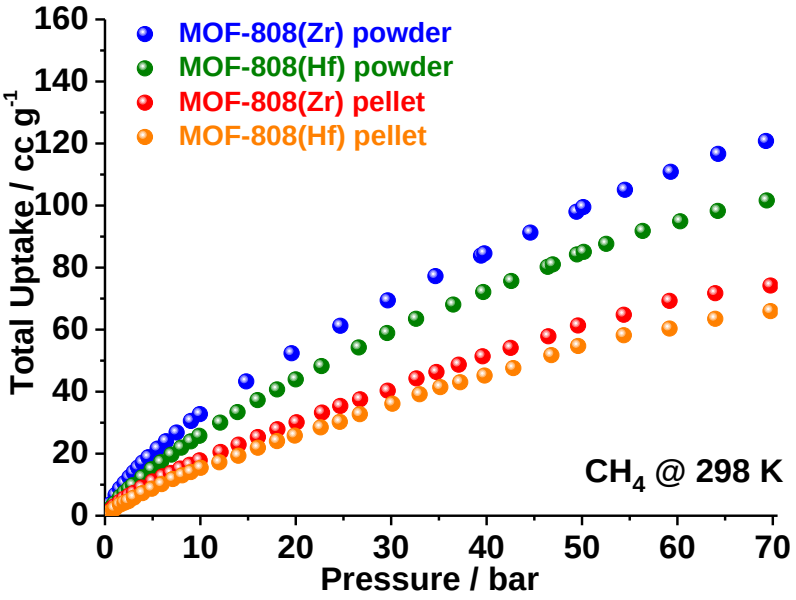

Figure S11. High-pressure gravimetric total CH_4 sorption isotherms of MOF-808 powder and pellet at 298 K.

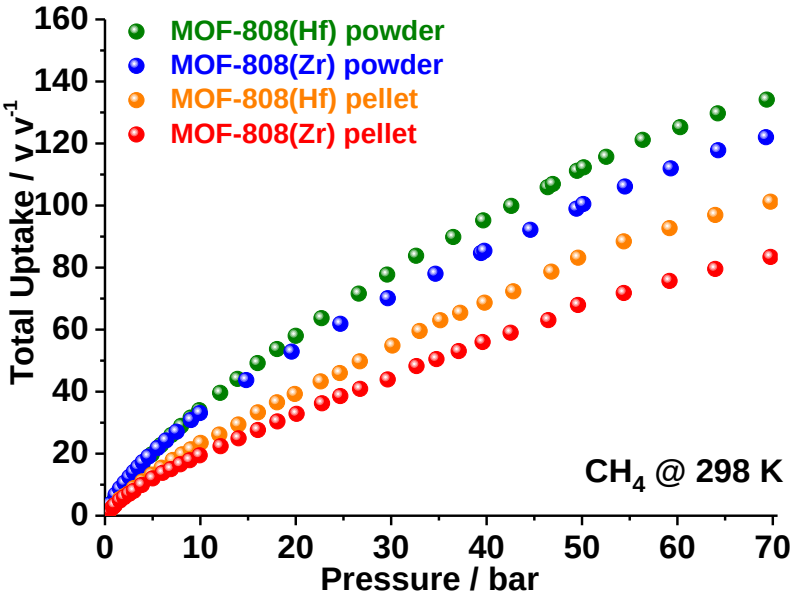

Figure S12. High-pressure volumetric total CH4 sorption isotherms of MOF-808 powder and pellet at 298 K. Volumetric uptake capacities are calculated by tap and pellet densities, respectively.

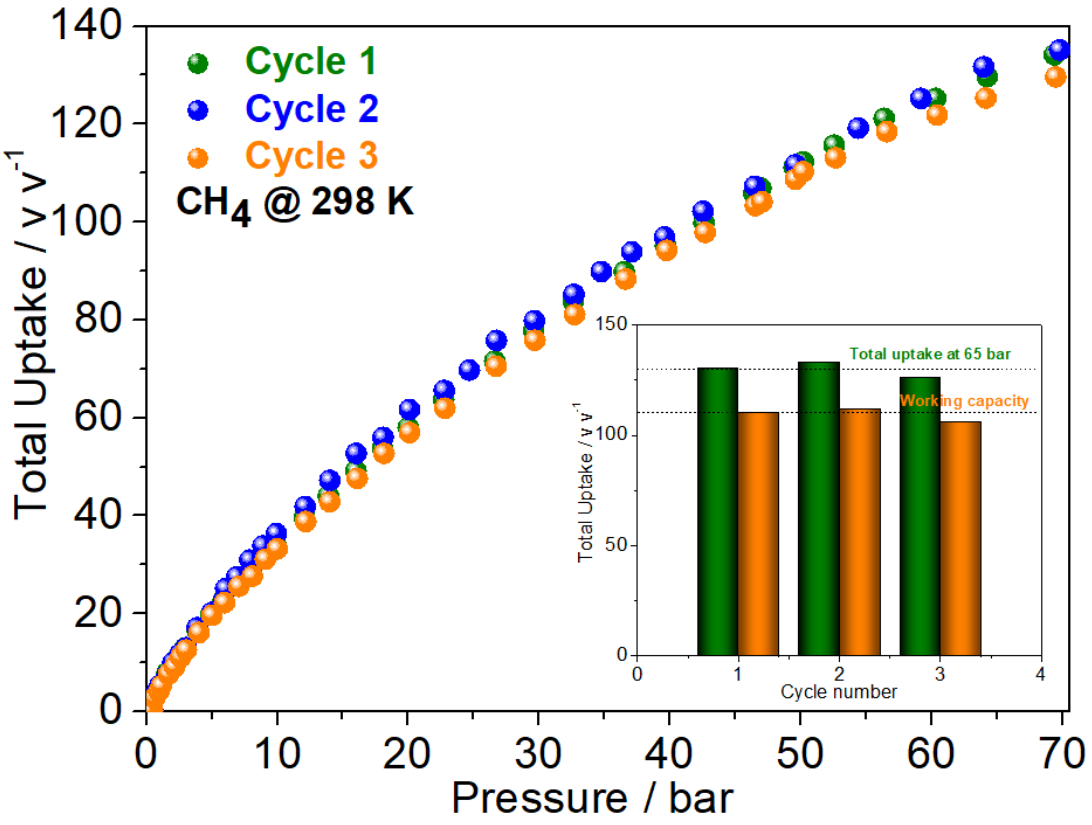

Figure S13. Total volumetric methane uptake isotherms of MOF-808(Hf) over 3 cycles, indicating no noticeable sample degradation within 3 continuous sorption cycles. The inset shows the variation of the total uptake at 65 bar and working capacity of 5.8–65 bar versus cycle number.

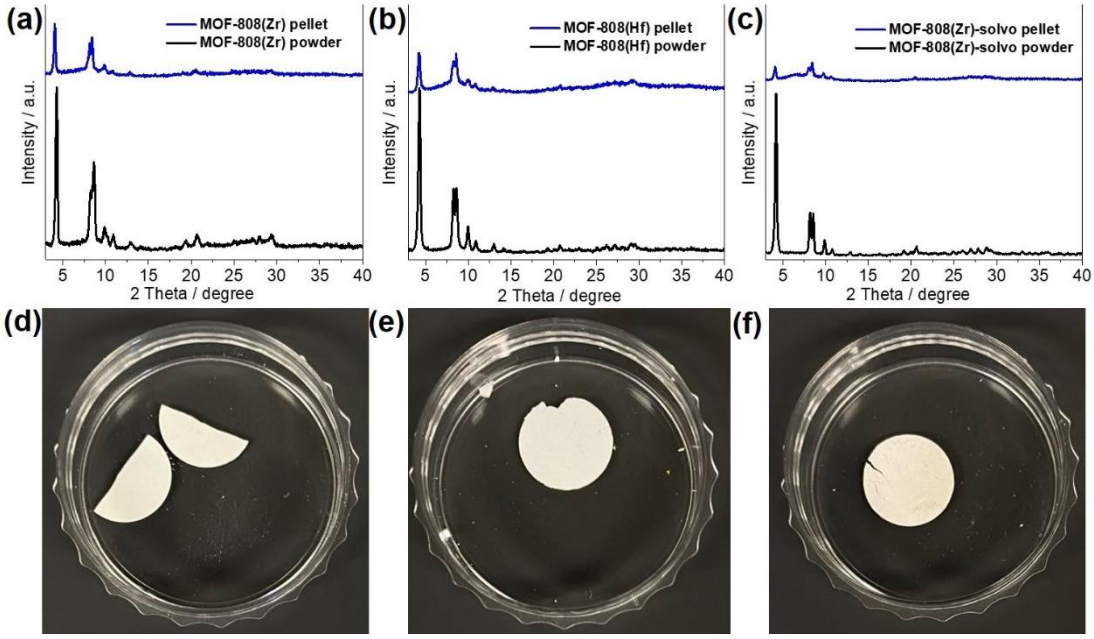

Figure S14. PXRD patterns (a-c) and optical images (d-f) of MOF-808 pellets (diameter: 12 mm): (a, d) MHT synthesized MOF-808(Zr); (b, e) MHT synthesized MOF-808(Hf); (c, f) solvothermally synthesized MOF-808(Zr).

Table S1. Summary of MOF-808(Hf) synthesis in the literature.

Year	Synthesis condition	BET surface area (m^2/g)	Pore volume	Application	Reference
2016	FA/DMF at 100 ºC for 3 days	1200	-	Styrene oxide ring-opening reaction	[2]
2017	FA/DMF at 120 ºC for 3 days	1340	-	Benzoxazole synthesis	[3]
2018	FA/DMF at 100 ºC for 3 days	458	0.3	Meerwein–Ponndorf–Verley reduction	[4]
2018	FA/DMF at 100 ºC for 3 days	458	0.3	Meerwein–Ponndorf–Verley reduction	[5]
2018	FA/DMF at 100 ºC for 3 days	1201	-	Imine synthesis	[6]
2020	FA/H_2O at 100 ºC for 12 h	1210	0.69	Gas storage	This work

Table S2. Optimization in the MHT synthesis of MOF-808.

Modulator	$ZrCl_4$ / $HfCl_4$ (g, 5.1 mmol)	BTC (g, 5 mmol)	Molar ratio (modulator to ligand)	Relative XRD crystallinity
AA	1.2/1.6	1.05	17	-
	1.2/1.6	1.05	35	-
	1.2/1.6	1.05	70	-
	1.2/1.6	1.05	105	-
	1.2/1.6	1.05	140	-
FA	1.2/1.6	1.05	26	-
	1.2/1.6	1.05	53	~20%
	1.2/1.6	1.05	106	100%
	1.2/1.6	1.05	159	~60%
	1.2/1.6	1.05	212	—
TFA	1.2/1.6	1.05	13	-
	1.2/1.6	1.05	26	~10%
	1.2/1.6	1.05	52	~50%
	1.2/1.6	1.05	78	~20%
	1.2/1.6	1.05	104	-

"-" indicates amorphous products.

Table S3. Summary of porosity, gas uptake, and Q_{st} values of MOF-808.

		MOF-808(Zr)	MOF-808(Hf)
BET SA[a)]		1650	1210
Langmuir SA[a)]		2100	1620
Pore volume[b)]		0.81	0.69
Pore size[c)]		6.9 & 19	6.9 & 16
CO_2 uptake[d)]	298 K	1.61	1.45
	273 K	2.81	2.40
H_2 uptake[d)]	77 K	6.65	5.84
	87 K	4.22	2.92
CH_4 uptake[d)]	298 K	0.39	0.29
	273 K	0.57	0.52
Q_{st} of CO_2[e)]		23.2	25.3
Q_{st} of H_2[e)]		6.6	8.2
Q_{st} of CH_4[e)]		15.8	16.5
Metal/carbon molar ratio[f)]		0.263	0.259

[a)] $m^2 g^{-1}$; [b)] $cm^3 g^{-1}$, [c)] Å, [d)] mmol g^{-1}, [e)] kJ mol^{-1}, [f)] EA analysis.

Table S4. Summary of gravimetric and volumetric methane working capacities of common porous materials.

Materials	S_{BET} (m^2 g^{-1})	Initial Q_{st} (kJ/mol)	Gravimetric working capacity (g g^{-1})[a)]	Volumetric working capacity (cm^3 (STP) cm^{-3})[a)]	Volumetric capacity at 65 bar (cm^3 (STP) cm^{-3})
MOF-5(Zn)[7]	3320	-	0.196	166	182
UTSA-76a(Cu)[8]	2820	15.4	0.201	197	257
$_{mono}$HKUST-1[9]	1193	-	0.121	185	259
HKUST-1(Cu)[10]	1850	17.0	0.154	190	267
NOTT-101a(Cu)[11]	2805	15.5	0.189	181	237
PCN-14(Cu)[10]	2000	19.0	0.200	157	230
MOF-519(Al)[7]	2400	14.6	0.157	210	260
Al-SOC-MOF-1[12]	5585	11.0	0.370	176	197
UTSA-110(Cu)[13]	3241	14.5	0.226	190	241
MOF-905(Zn)[14]	3490	11.7	0.241	181	206
Co(bdp)[15]	2780	73.4	-	197	205
NJU-Bai-43(Cu)[16]	3090	17.8	0.221	198	254
DUT-49(Cu)[17]	5476	-	0.36	157	179
MAF-38(Zn)[18]	2022	21.6	0.176	187	263
MFM-115(Cu)[19]	3394	16.3	0.223	191	238
BUT-22(Al)[20]	4380	12	0.295	158	182
Fe(pbpta)[21]	4937	22.3	0.37	192	219
FJU-101a(Cu)[22]	1909	17.3	0.172	144	212

MOF-74(Mg)[23]	1542	18.5	0.111	142	230
PCN-68(Cu)[24]	5100	15.2	0.216	107	125
COP-150[25]	120	-	0.137	30	38
CBZ-1[26]	1622	18.5	0.145	95	126
PAF-1[26]	4784	16.6	0.328	120	145
F400[27]	1070	-	0.11	60	144
LMA738[27]	3290	-	0.30	174	221
Zeolite 13X (estimated)[28]	-	115.3	0.067	105	164
UiO-67(Zr)[29]	1575	13.4	0.146	145	183
NU-1100(Zr)[30]	4020	11	0.240	156	180
NU-1501(Al)[31]	7310	9.7	0.370	147	163
MIL-53(Al)-OH[32]	1283	-	0.118	164	217
MIL-53(Al)-$(OH)_2$[32]	1193	-	0.055	71	86
$_{mono}$UiO-66(Zr)[33]	982	-	0.118	172	211
UiO-66(Zr)[34]	970	15.8	0.055	97	156
MOF-808(Hf) (pellets)	1210	16.5	0.064 (0.041)	110 (86)	130 (98)
MOF-808(Zr) (pellets)	1650	15.8	0.074 (0.044)	96 (69)	118 (81)

[a)] Working capacity is defined as the difference in the total uptake between 65 and 5.8 bar.

References

(1) Traina, K.; Cloots, R.; Bontempi, S.; Lumay, G.; Vandewalle, N.; Boschini, F., Flow abilities of powders and granular materials evidenced from dynamical tap density measurement. *Powder Technol.* **2013,** *235*, 842-852. DOI: 10.1016/j.powtec.2012.11.039.

(2) Liu, Y.; Klet, R. C.; Hupp, J. T.; Farha, O., Probing the correlations between the defects in metal–organic frameworks and their catalytic activity by an epoxide ring-opening reaction. *Chem. Commun.* **2016,** *52* (50), 7806-7809. DOI: 10.1039/C6CC03727E.

(3) Nguyen, L. H. T.; Nguyen, T. T.; Nguyen, H. L.; Doan, T. L. H.; Tran, P. H., A new superacid hafnium-based metal–organic framework as a highly active heterogeneous catalyst for the synthesis of benzoxazoles under solvent-free conditions. *Catal. Sci. Technol.* **2017,** *7* (19), 4346-4350. DOI: 10.1039/C7CY01668A.

(4) Rojas-Buzo, S.; García-García, P.; Corma, A., Hf-based metal–organic frameworks as acid–base catalysts for the transformation of biomass-derived furanic compounds into chemicals. *Green Chem.* **2018,** *20* (13), 3081-3091. DOI: 10.1039/C8GC00806J.

(5) Rojas-Buzo, S.; García-García, P.; Corma, A., Catalytic Transfer Hydrogenation of Biomass-Derived Carbonyls over Hafnium-Based Metal–Organic Frameworks. *ChemSusChem* **2018,** *11* (2), 432-438. DOI: 10.1002/cssc.201701708.

(6) Prasad, R. R. R.; Dawson, D. M.; Cox, P. A.; Ashbrook, S. E.; Wright, P. A.; Clarke, M. L., A Bifunctional MOF Catalyst Containing Metal–Phosphine and Lewis Acidic Active Sites. *Chem. Eur. J.* **2018,** *24* (57), 15309-15318. DOI: 10.1002/chem.201803094.

(7) Gándara, F.; Furukawa, H.; Lee, S.; Yaghi, O. M., High Methane Storage Capacity in Aluminum Metal–Organic Frameworks. *J. Am. Chem. Soc.* **2014,** *136* (14), 5271-5274. DOI: 10.1021/ja501606h.

(8) Li, B.; Wen, H.-M.; Wang, H.; Wu, H.; Tyagi, M.; Yildirim, T.; Zhou, W.; Chen, B., A Porous Metal–Organic Framework with Dynamic Pyrimidine Groups Exhibiting Record High Methane Storage Working Capacity. *J. Am. Chem. Soc.* **2014,** *136* (17), 6207-6210. DOI: 10.1021/ja501810r.

(9) Tian, T.; Zeng, Z.; Vulpe, D.; Casco, M. E.; Divitini, G.; Midgley, P. A.; Silvestre-Albero, J.; Tan, J.-C.; Moghadam, P. Z.; Fairen-Jimenez, D., A sol–gel monolithic metal–organic framework with enhanced methane uptake. *Nat. Mater.* **2018,** *17*, 174-179. DOI: 10.1038/nmat5050.

(10) Peng, Y.; Krungleviciute, V.; Eryazici, I.; Hupp, J. T.; Farha, O. K.; Yildirim, T., Methane Storage in Metal–Organic Frameworks: Current Records, Surprise Findings, and Challenges. *J. Am. Chem. Soc.* **2013,** *135* (32), 11887-11894. DOI: 10.1021/ja4045289.

(11) He, Y.; Zhou, W.; Yildirim, T.; Chen, B., A series of metal–organic frameworks with high methane uptake and an empirical equation for predicting methane storage capacity. *Energy Environ. Sci.* **2013,** *6* (9), 2735-2744. DOI: 10.1039/C3EE41166D.

(12) Alezi, D.; Belmabkhout, Y.; Suyetin, M.; Bhatt, P. M.; Weseliński, Ł. J.; Solovyeva, V.; Adil, K.; Spanopoulos, I.; Trikalitis, P. N.; Emwas, A.-H.; Eddaoudi, M., MOF Crystal Chemistry Paving the Way to Gas Storage Needs: Aluminum-Based soc-MOF for CH_4, O_2, and CO_2 Storage. *J. Am. Chem. Soc.* **2015,** *137* (41), 13308-13318. DOI: 10.1021/jacs.5b07053.

(13) Wen, H.-M.; Li, B.; Li, L.; Lin, R.-B.; Zhou, W.; Qian, G.; Chen, B., A Metal–Organic Framework with Optimized Porosity and Functional Sites for High Gravimetric and Volumetric Methane Storage Working Capacities. *Adv. Mater.* **2018,** *30* (16), 1704792. DOI: 10.1002/adma.201704792.

(14) Jiang, J.; Furukawa, H.; Zhang, Y.-B.; Yaghi, O. M., High Methane Storage Working Capacity in Metal–Organic Frameworks with Acrylate Links. *J. Am. Chem. Soc.* **2016,** *138* (32), 10244-10251. DOI: 10.1021/jacs.6b05261.

(15) Mason, J. A.; Oktawiec, J.; Taylor, M. K.; Hudson, M. R.; Rodriguez, J.; Bachman, J. E.; Gonzalez, M. I.; Cervellino, A.; Guagliardi, A.; Brown, C. M.; Llewellyn, P. L.; Masciocchi, N.; Long, J. R., Methane storage in flexible metal–organic frameworks with intrinsic thermal management. *Nature* **2015,** *527* (7578), 357-361. DOI: 10.1038/nature15732.

(16) Zhang, M.; Zhou, W.; Pham, T.; Forrest, K. A.; Liu, W.; He, Y.; Wu, H.; Yildirim, T.; Chen, B.; Space, B.; Pan, Y.; Zaworotko, M. J.; Bai, J., Fine Tuning of MOF-505 Analogues To Reduce Low-Pressure Methane Uptake and Enhance Methane Working Capacity. *Angew. Chem. Int. Ed.* **2017,** *56* (38), 11426-11430. DOI: 10.1002/anie.201704974.

(17) Stoeck, U.; Krause, S.; Bon, V.; Senkovska, I.; Kaskel, S., A highly porous metal–organic framework, constructed from a cuboctahedral super-molecular building block, with exceptionally high methane uptake. *Chem. Commun.* **2012,** *48* (88), 10841-10843. DOI: 10.1039/C2CC34840C.

(18) Lin, J.-M.; He, C.-T.; Liu, Y.; Liao, P.-Q.; Zhou, D.-D.; Zhang, J.-P.; Chen, X.-M., A Metal–Organic Framework with a Pore Size/Shape Suitable for Strong Binding and Close Packing of Methane. *Angew. Chem. Int. Ed.* **2016,** *55* (15), 4674-4678. DOI: 10.1002/anie.201511006.

(19) Yan, Y.; Kolokolov, D. I.; da Silva, I.; Stepanov, A. G.; Blake, A. J.; Dailly, A.; Manuel, P.; Tang, C. C.; Yang, S.; Schröder, M., Porous Metal–Organic Polyhedral Frameworks with Optimal Molecular Dynamics and Pore Geometry for Methane Storage. *J. Am. Chem. Soc.* **2017,** *139* (38), 13349-13360. DOI: 10.1021/jacs.7b05453.

(20) Wang, B.; Zhang, X.; Huang, H.; Zhang, Z.; Yildirim, T.; Zhou, W.; Xiang, S.; Chen, B., A microporous aluminum-based metal-organic framework for high methane, hydrogen, and carbon dioxide storage. *Nano Res.* **2020**, 10.1007/s12274-020-2713-0. DOI: 10.1007/s12274-020-2713-0.

(21) Verma, G.; Kumar, S.; Vardhan, H.; Ren, J.; Niu, Z.; Pham, T.; Wojtas, L.; Butikofer, S.; Echeverria Garcia, J. C.; Chen, Y.-S.; Space, B.; Ma, S., A robust soc-MOF platform exhibiting high gravimetric uptake and volumetric deliverable capacity for on-board methane storage. *Nano Res.* **2020**, 10.1007/s12274-020-2794-9. DOI: 10.1007/s12274-020-2794-9.

(22) Ye, Y.; Lin, R.-B.; Cui, H.; Alsalme, A.; Zhou, W.; Yildirim, T.; Zhang, Z.; Xiang, S.; Chen, B., A microporous metal–organic framework with naphthalene diimide groups for high methane storage. *Dalton Trans.* **2020,** *49* (12), 3658-3661. DOI: 10.1039/C9DT01911A.

(23) Mason, J. A.; Veenstra, M.; Long, J. R., Evaluating metal-organic frameworks for natural gas storage. *Chem. Sci.* **2014,** *5* (1), 32-51. DOI: 10.1039/C3SC52633J.

(24) Yuan, D.; Zhao, D.; Sun, D.; Zhou, H.-C., An Isoreticular Series of Metal–Organic Frameworks with Dendritic Hexacarboxylate Ligands and Exceptionally High Gas-Uptake Capacity. *Angew. Chem. Int. Ed.* **2010,** *49* (31), 5357-5361. DOI: 10.1002/anie.201001009.

(25) Rozyyev, V.; Thirion, D.; Ullah, R.; Lee, J.; Jung, M.; Oh, H.; Atilhan, M.; Yavuz, C. T., High-capacity methane storage in flexible alkane-linked porous aromatic network polymers. *Nat. Energy* **2019,** *4* (7), 604-611. DOI: 10.1038/s41560-019-0427-x.

(26) Bracco, S.; Piga, D.; Bassanetti, I.; Perego, J.; Comotti, A.; Sozzani, P., Porous 3D polymers for high pressure methane storage and carbon dioxide capture. *J. Mater. Chem. A* **2017,** *5* (21), 10328-10337. DOI: 10.1039/C7TA00934H.

(27) Casco, M. E.; Martínez-Escandell, M.; Gadea-Ramos, E.; Kaneko, K.; Silvestre-Albero, J.; Rodríguez-Reinoso, F., High-Pressure Methane Storage in Porous Materials: Are Carbon Materials in the Pole Position? *Chem. Mater.* **2015,** *27* (3), 959-964. DOI: 10.1021/cm5042524.

(28) Cavenati, S.; Grande, C. A.; Rodrigues, A. E., Adsorption Equilibrium of Methane, Carbon Dioxide, and Nitrogen on Zeolite 13X at High Pressures. *J. Chem. Eng. Data* **2004,** *49* (4), 1095-1101. DOI:

10.1021/je0498917.
(29) Yang, Q.; Guillerm, V.; Ragon, F.; Wiersum, A. D.; Llewellyn, P. L.; Zhong, C.; Devic, T.; Serre, C.; Maurin, G., CH_4 storage and CO_2 capture in highly porous zirconium oxide based metal–organic frameworks. *Chem. Commun.* **2012,** *48* (79), 9831-9833. DOI: 10.1039/C2CC34714H.
(30) Gutov, O. V.; Bury, W.; Gomez-Gualdron, D. A.; Krungleviciute, V.; Fairen-Jimenez, D.; Mondloch, J. E.; Sarjeant, A. A.; Al-Juaid, S. S.; Snurr, R. Q.; Hupp, J. T.; Yildirim, T.; Farha, O. K., Water-Stable Zirconium-Based Metal–Organic Framework Material with High-Surface Area and Gas-Storage Capacities. *Chem. Eur. J.* **2014,** *20* (39), 12389-12393. DOI: 10.1002/chem.201402895.
(31) Chen, Z.; Li, P.; Anderson, R.; Wang, X.; Zhang, X.; Robison, L.; Redfern, L. R.; Moribe, S.; Islamoglu, T.; Gómez-Gualdrón, D. A.; Yildirim, T.; Stoddart, J. F.; Farha, O. K., Balancing volumetric and gravimetric uptake in highly porous materials for clean energy. *Science* **2020,** *368* (6488), 297. DOI: 10.1126/science.aaz8881.
(32) Kundu, T.; Shah, B. B.; Bolinois, L.; Zhao, D., Functionalization-Induced Breathing Control in Metal–Organic Frameworks for Methane Storage with High Deliverable Capacity. *Chem. Mater.* **2019,** *31* (8), 2842-2847. DOI: 10.1021/acs.chemmater.8b05332.
(33) Connolly, B. M.; Aragones-Anglada, M.; Gandara-Loe, J.; Danaf, N. A.; Lamb, D. C.; Mehta, J. P.; Vulpe, D.; Wuttke, S.; Silvestre-Albero, J.; Moghadam, P. Z.; Wheatley, A. E. H.; Fairen-Jimenez, D., Tuning porosity in macroscopic monolithic metal-organic frameworks for exceptional natural gas storage. *Nat. Commun.* **2019,** *10* (1), 2345. DOI: 10.1038/s41467-019-10185-1.
(34) Wiersum, A. D.; Chang, J.-S.; Serre, C.; Llewellyn, P. L., An Adsorbent Performance Indicator as a First Step Evaluation of Novel Sorbents for Gas Separations: Application to Metal–Organic Frameworks. *Langmuir* **2013,** *29* (10), 3301-3309. DOI: 10.1021/la3044329.